Hindawi
Advances in Condensed Matter Physics
Volume 2021, Article ID 5544835, 7 pages
https://doi.org/10.1155/2021/5544835

Research Article

Microwave Vitrification of Uranium Tailings: Microstructure and Mechanical Property

Wei Wei,[1] Keyou Shi,[1] Yupeng Xie,[1] Shoufu Yu,[2] Jiawei Li,[1] Min Chen,[1] Zengming Tang,[1] Ailian Zhu,[1] Qiucai Zhang ,[1,3,4] and Yong Liu [1,3,4]

[1]*School of Resource & Environment and Safety Engineering, University of South China, Hengyang 421001, China*
[2]*School of Nuclear Science and Technology, University of South China, Hengyang 421001, China*
[3]*Hunan Province Engineering Technology Research Center of Uranium Tailings Treatment, Hengyang 421001, China*
[4]*Hunan Province Engineering Research Center of Radioactive Control Technology in Uranium Mining and Metallurgy, Hengyang 421001, China*

Correspondence should be addressed to Qiucai Zhang; zqiucai@163.com and Yong Liu; liuyong81668@163.com

Received 29 January 2021; Revised 15 March 2021; Accepted 27 March 2021; Published 19 April 2021

Academic Editor: Sefer Bora Lisesivdin

In this work, the dense glass matrix of uranium tailings was successfully fabricated via microwave sintering process with Na_2CO_3 as a sintering aid. The effects of Na_2CO_3 additive and sintering temperature on the microstructure and mechanical properties of as-prepared solids were systematically investigated. XRD results confirmed the vitrified forms can be achieved at 1200°C within 30 min with 20 wt.% Na_2CO_3 addition. Importantly, the Na_2CO_3 additive significantly reduced the firing temperature from 1500°C to 1200°C and promoted densification. FT-IR analysis demonstrated that the main characteristic peaks of the sintered samples were attributed to the vibration of Si-O-Si. Microstructural studies presented the homogeneous distribution of glass phases. The results of mechanical properties of the sintered forms show that bulk density and Vickers hardness increased with increasing Na_2CO_3 content as well as sintering temperature, and the highest bulk density (2.45 ± 0.01 g/cm^3) and Vickers hardness (823 ± 25 HV) were obtained at the temperature of 1300°C with 20 wt.% Na_2CO_3 addition, the heating rate of 20°C/min, and the soaking time of 30 min. It implied that the combination of microwave sintering with the appropriate addition of Na_2CO_3 would provide an efficient method for the immobilization of radionuclides in uranium tailings.

1. Introduction

With the development of the nuclear industry, the demand for uranium resources increases dramatically, which resulted in a significant increase in uranium tailings [1]. The main pollution in uranium tailings is actinide nuclides and other radionuclides, whose disposal methods are necessary for preventing their migration into water or air [2, 3]. The migration of radioactive contamination into the surrounding would pollute the environment and pose a great threat to human health [1, 4–7]. Although the average grade of radionuclides content is slightly low, the potential harm to human health cannot be ignored [8, 9]. Therefore, it is urgent to find an efficient and reliable immobilization method to safely dispose of radionuclides in uranium tailings.

For the remediation of the uranium tailings pond, physical remediation, chemical remediation, microbial remediation, and phytoremediation have been considered [10]. The physical remediation [11, 12] method requires simple equipment at a low cost, which can be considered as efficient treatment. The chemical remediation [9, 13, 14] method has expensive costs for large numbers of chemical reagents, which could result in secondary pollution. The microbial remediation and phytoremediation method [15–19] have low cost, while the strong biological selectivity limits their application. Meanwhile, the posttreatment of microorganisms and plants might also cause secondary pollution.

In situ vitrification (ISV) technology is commonly considered as an effective alternative to physical remediation to immobilize radionuclides in radioactively contaminated

soil with high chemical durability [20–23]. It used Joule heating to convert radioactively contaminated soil into the glass in which most radionuclides can be fixed [24–26]. Conventional pressureless sintering, spark plasma sintering (SPS), and microwave sintering are the most commonly used methods employed for heating materials [27]. The traditional joule heating method requires a long heating time, and the uniformity of the solidification is hard to obtain [25]. SPS method could achieve high-density parts of materials at lower sintering temperatures, but it needs to be carried out by applying pressure [28]. Compared with other sintering methods, microwave sintering is a highly efficient heating method without pressure in which the material is heated by the dielectric loss of the material itself, rather than gradually transferring heat to the inner of the material by heating the surface of the material [29]. Therefore, a rapid vitrification method and good homogeneity of the cured matrix are the key challenges for the solidified uranium tailings.

In this study, microwave sintering has been employed to immobilize the radionuclides in uranium tailings. The Na_2CO_3 was introduced as a sintering additive to lower the sintering temperature and promote densification. Effects of Na_2CO_3 addition and sintering temperature on phase composition, microstructure, density, and Vickers hardness were investigated systematically. As a result of this work, high-density and hardness vitrified forms with homogeneously distributed amorphous glass phases were successfully fabricated. The outcomes provide a theoretical basis for the researchers to solidify radionuclides and have important guiding significance for the engineering application of the beach surface of the uranium tailings reservoir in the later stage.

2. Experimental

2.1. Preparation. The raw uranium tailings sample was collected from a uranium tailings pond in Hunan Province, China, ranging from −10 cm to −30 cm in depth, and the cladding was taken from the surface varying from 0 cm to −10 cm in depth. After being pretreated at 105°C for 24 h to remove the absorptive water, the raw uranium tailings and surface cladding were thoroughly mixed in an agate mortar in a 1 : 1 mass ratio and sifted through a 200-mesh sieve. The chemical compositions of the uranium tailings and surface cladding determined by X-ray fluorescence (XRF, Axios, Netherlands) are listed in Table 1.

In order to reduce the sintering temperature, the sodium carbonate powder (AR grade) was proposed as a sintering aid. The doping gradient of Na_2CO_3 was set to 5%, from 0% to 20%. Each sample was weighted at 6.000 g, and then, the sample consisting of sodium carbonate, uranium tailings, and surface cladding was further mixed in a mortar using alcohol (AR grade) as a medium. Microwave sintering was carried out for all samples. During this process, the sample held in a 10 mL alumina crucible was placed on some SiC plates which were used to act as a preheater for auxiliary heating [30–32]. Samples with varying Na_2CO_3 contents were sintered at 1000°C, 1100°C, 1200°C, and 1300°C, respectively, for 30 min in air atmosphere. The heating rate was set to 30°C/min, while the temperature was below 600°C. Then, the heating rate was set to 20°C/min in the temperature range of 600°C to 900°C. After 900°C, the target firing temperature was reached with the heating rate of 10°C/min. The sintered specimens were naturally cooled to room temperature. The entire microwave sintered process real-time power and temperature output varied with time are depicted in Figure 1. From the sintered sample in Figure 2, we can see that, without adding Na_2CO_3, the sample contracted with the increase of temperature. When the sintering temperature is 1000°C, a small amount of amorphous phase appears with the increase of Na_2CO_3 content. When the sintering temperature is increased to accelerate the material reaction, it can be seen that the samples of 1200°C and 1300°C with 20 wt.% Na_2CO_3 addition are completely glass.

2.2. Characterization. The phase structure of the sintered compacts was examined by X-ray diffraction (XRD, Ultima IV, Japan) using Cu-Kα radiation ($\lambda = 1.5406$ Å) at 40 kV and 40 mA in the 10°–90° (2θ) range with a scan speed of 5°/min. The detailed structure information was collected by Fourier transform infrared spectrometer (FT-IR, IRPrestige-21, American). The microstructure of the vitrified forms was observed by scanning electron microscopy (SEM, EVO 18, Germany). The bulk density of samples was measured using a high-precision solid-liquid dual-use density tester (DE-200T, China) by the Archimedes method with distilled water as the liquid medium. The Vickers hardness of the samples was obtained by using a standard microindentation device (HVS-1000AV, China) with 200 g load.

3. Result and Discussion

3.1. XRD Analysis. Figure 3(a) shows the XRD patterns of samples with a series of Na_2CO_3-doping contents (0 wt.%, 5 wt.%, 10 wt.%, 15 wt.%, and 20 wt.%) calcined at 1200°C for 30 min. It can be seen that the main phases of pure uranium tailings cladding complexes are quartz and $NaAlSi_3O_8$. With the Na_2CO_3 dosage amount increasing, the intensity of diffraction peaks of SiO_2 and $NaAlSi_3O_8$ gradually decreased. Furthermore, the Na_2CO_3 contents amount to 20 wt.%, and no obvious crystal diffraction peaks can be observed. It implies that the introduction of Na_2CO_3 promoted the glass phase transformation.

To further confirm the optimal sintering temperature, a series of samples dopped 20 wt.% were cured at different temperatures (1000°C, 1100°C, 1200°C, and 1300°C) for 30 min. Figure 3(b) presents the XRD pattern of the above samples. As can be seen, the glass with the presence of crystalline phases can be found when the firing temperatures are in the range of 1000°C to 1100°C. When the temperature is 1000°C, the two main phases of the samples are also quartz and slight $NaAlSi_3O_8$. As the temperature increased, the intensity of $NaAlSi_3O_8$-related diffraction peaks decreased rapidly, while that of quartz reduced gradually. At 1100°C, the phase of $NaAlSi_3O_8$ disappeared, and until 1200°C, no SiO_2-related peaks were observed. It indicates that the

Table 1: Chemical compositions (wt.%) of uranium tailings and surface cladding determined by XRF.

Compound	SiO_2	Al_2O_3	K_2O	Fe_2O_3	SO_3	Na_2O	F	CaO	MgO	TiO_2	P_2O_5	U_3O_8
Uranium tailings	79.02	10.11	3.56	1.96	1.93	0.83	0.83	0.54	0.37	0.27	0.21	0.0045
Surface cladding	47.97	31.68	2.74	13.70	0.25	0.16	0.34	—	1.02	1.49	0.20	—

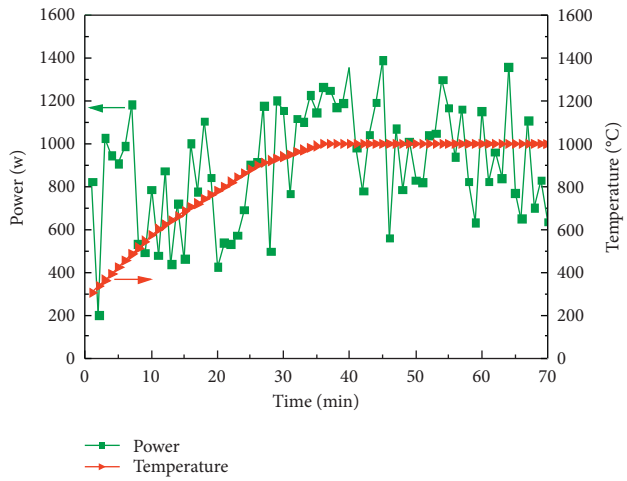

Figure 1: The real-time power and temperature output as a function of time.

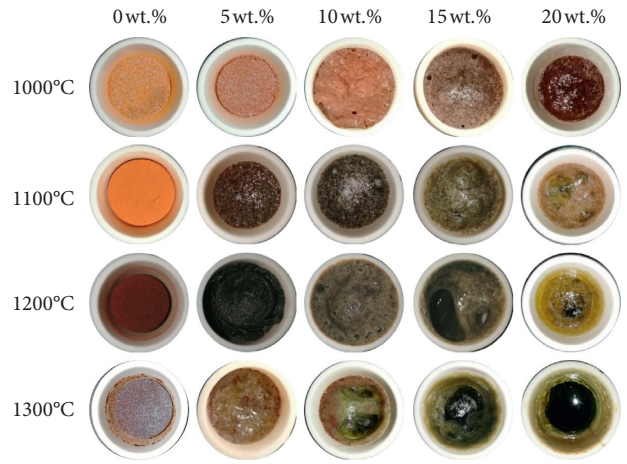

Figure 2: Samples sintered.

samples with 20 wt.% Na_2CO_3-doping had been vitrified almost completely at 1200°C for 30 min.

3.2. FT-IR Analysis. To further detect the detailed structure of sintered samples, the FT-IR technique was utilized. Figure 4(a) exhibits the FT-IR spectra of the sintered samples with various contents of Na_2CO_3 obtained at 1200°C for 30 min. It can be intuitively seen that the main absorption bands of the solidified samples were concentrated in the range of 400–1800 cm^{-1} [33]. Generally, the absorption peaks near 474 cm^{-1} and 786 cm^{-1} were attributed to the bending vibration of Si-O-Si and the symmetrical telescopic vibration peak of Si-O bonds, respectively [34]. The absorption peak near 584 was due to the Al-O bond. The strong and wide absorption peaks in the range of 800 cm^{-1}–1200 cm^{-1} were attributed to the antisymmetric stretching vibration of the Si-O-Si bond, which indicates that the glass network structure exists [35]. As the doping amount of Na_2CO_3 increased, the intensity of these absorption peaks increased, implying that the amorphous degree of sintered samples increased, which was in accordance with the XRD result. It is noteworthy that, with the dosage amount of Na_2CO_3 increasing, the absorption peaks near 1080 cm^{-1} became much flatter and shifted towards the lower wavenumber, indicating that the enhancement of the Si-O bond and amorphous degree. In addition, the weak absorption peaks at 1380 cm^{-1} and 1536 cm^{-1} were assigned to the bending vibration peak of $-CH_3$ and stretching vibration and bending vibration peak of –OH bonds, respectively [1]. These peaks of $-CH_3$ and –OH may be caused by the introduction of alcohol during the sample preparation just before characterization. On the other hand, Figure 4(b) demonstrates the FT-IR spectra of the samples 20 wt.% Na_2CO_3-doped sintered at the temperature range of 1000°C–1300°C. With the increase of temperature, the position of the main absorption peak of the solidified body has not changed, and the intensity of the absorption peak has decreased. This may be due to the gradual increase in the content of Na_2CO_3 decomposition into Na_2O, which promotes the fracture of Si-O bonds and thus plays the role of melting.

3.3. SEM Analysis. Figure 5 shows the SEM and EDS of uranium tailings doped 20% Na_2CO_3 solidified by microwave sintering at 1000°C and 1200°C. It can be seen from Figure 5(a) that when the microwave sintering temperature is 1000°C, the surface of uranium tailings doped with Na_2CO_3 was relatively uniform and smooth, but there were some voids on the surface, indicating that the solidified body is not dense at this time. Figure 5(c) shows the macromorphology of samples with 20 wt.% Na_2CO_3-doped before and after sintering at 1200°C. We can see that the loose uranium tailings mixture was transformed into dense glass and the volumes of samples reduced significantly after sintering. Compared with Figure 5(a), we can see that the surface of the microwave-cured body at 1200°C was smoother and there was no obvious void. In consequence, combined with the analysis results of XRD, the cured body at this time was vitreous. On the other hand, as displayed in Figures 5(b) and 5(d). The contents of the main elements (O, Na, Mg, Al, Si, and K) distributed in these figures were almost the same, and the analysis results are consistent with the XRF analysis results of uranium tailings. To sum up, when the doping amount of Na_2CO_3 is 20 wt.% and the microwave sintering temperature is 1200°C, uranium tailings can be sintered into dense vitreous surface.

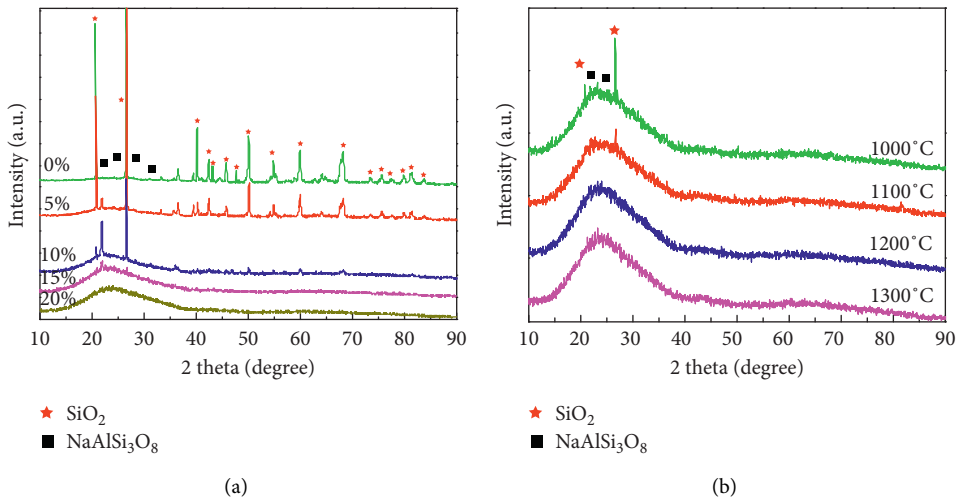

Figure 3: XRD patterns: (a) different Na_2CO_3 contents and (b) different temperatures.

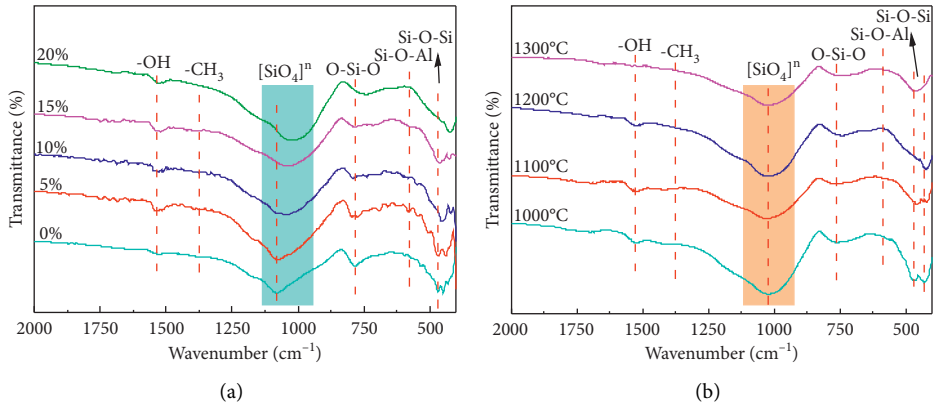

Figure 4: FT-IR spectra of samples: (a) different contents of Na_2CO_3 and (b) different temperatures.

3.4. Density and Porosity Analysis. Density and porosity are also important parameters to judge the quality of materials. Figure 6 studies the effects of temperature and Na_2CO_3 addition on the density and porosity of microwave-cured uranium tailings. As displayed in Figure 6(a), when the doping amount of Na_2CO_3 was 20 wt.%, the density of the microwave-cured body gradually increases with the increase in temperature. When the temperature was 1300°C, the density was 2.45 g/cm^3. In addition, the porosity gradually decreases with the increase in temperature. When the temperature was 1200°C, the porosity will basically be 0. As can be seen from Figure 6(b), when the temperature is 1200°C, the density of the microwave-curable body gradually increases with the increase of the doping amount of Na_2CO_3, while the porosity gradually decreases with the increase of the doping amount. When the doping amount of Na_2CO_3 is 20, the density is 2.40 g/cm^3 and the porosity is 0. Combining the analysis results of XRD and SEM-EDS, it can be seen that when the microwave sintering temperature was 1200°C and the Na_2CO_3 doping amount was 20 wt.%, uranium tailings can be sintered into a dense glass solidified body. Therefore, considering both the excellent performance of the microwave solidified body and the energy saving, the temperature of 1200°C and the Na_2CO_3 doping amount of 20 can be used as the best sintering process.

3.5. Vickers Hardness Analysis. As demonstrated in Figure 7, the Vickers hardness of samples sintered at various temperatures versus Na_2CO_3 doping amount was plotted to investigate the effect of Na_2CO_3 doping on the mechanical properties of the solidified matrix. At least five Vickers indentations were performed on different positions of each polished sample surface. The final values of hardness were based on their average [32]. The Vickers hardness exhibited a positive correlation with the density, as we recognized [36, 37]. The Vickers hardness of the sintered samples increased with the sintering temperature increasing. The hardness of samples had a slowdown growth trend from 1200°C to 1300°C, consistent with the trend of the density. Moreover, the hardness reached a relatively high value of 781 HV and 823 HV for the samples with the addition of 20 wt.% Na_2CO_3 sintered at 1200°C and 1300°C, respectively. Based

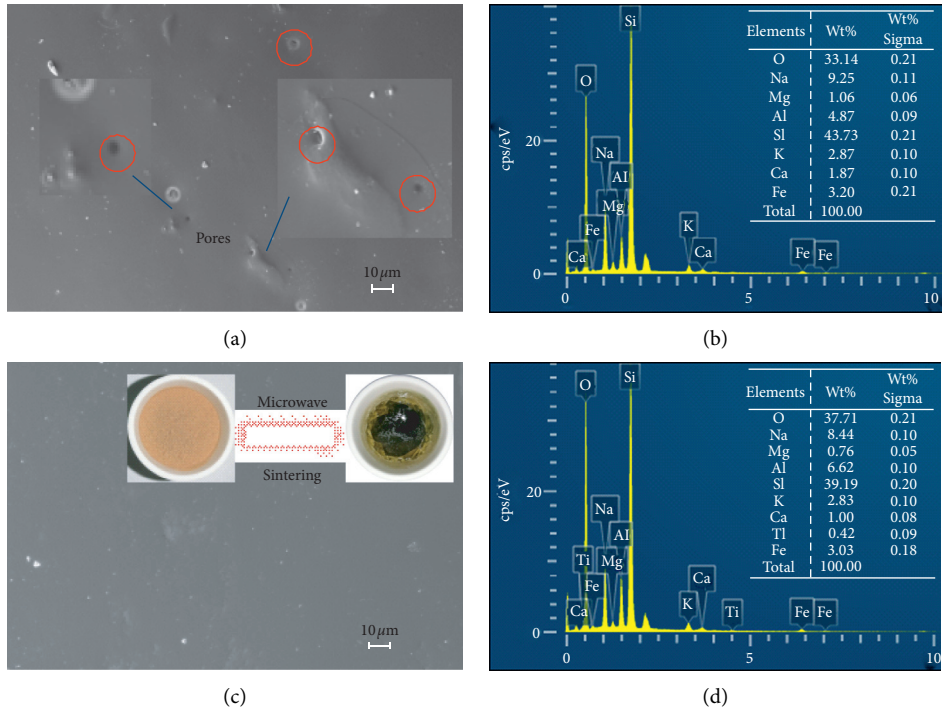

Figure 5: SEM image and EDS spectra of solidified forms at 1000°C (a, b) and 1200°C (c, d), respectively.

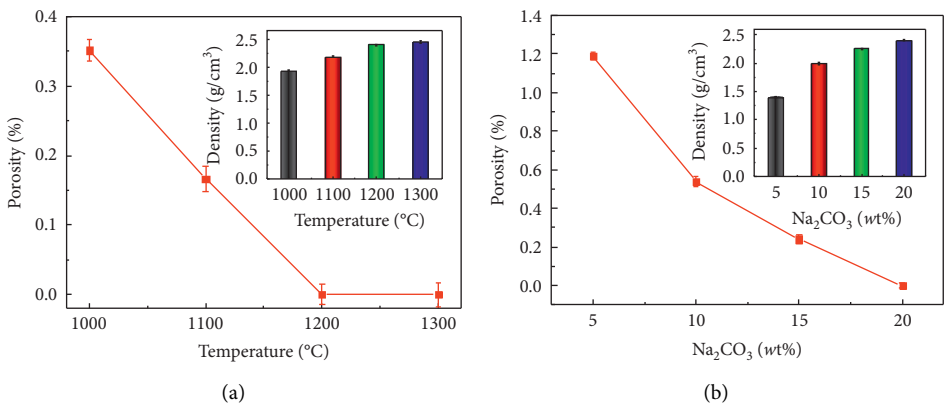

Figure 6: The influence of sintering temperature (a) and the effect of Na_2CO_3 (b) doping on the density and porosity of solidified body.

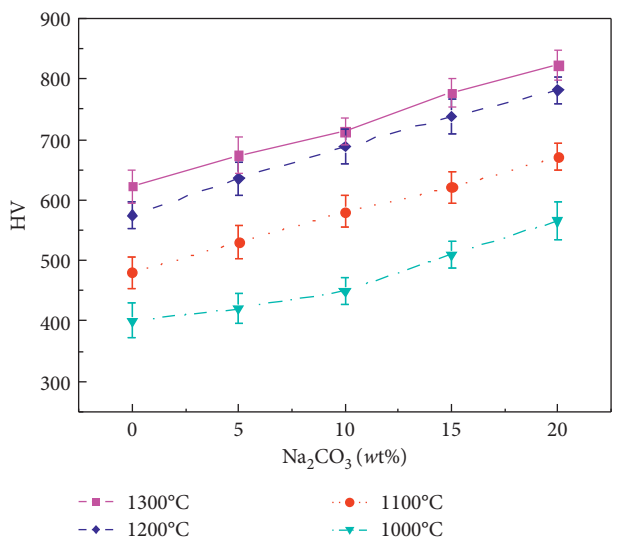

Figure 7: Vickers hardness of different Na_2CO_3 addition under different temperatures.

on the above analysis, it can be concluded that the uranium tailings mixture doped 20 wt.% Na_2CO_3 sintered at 1200°C showed excellent performance, regardless of the density or Vickers hardness.

4. Conclusion

The uranium tailings mixtures (1 : 1 mass ratio) were successfully vitrified by microwave sintering at 1200°C within 30 min with the addition of Na_2CO_3. The effects of Na_2CO_3 dopant on the microstructure and densification behavior of as-prepared solids were systematically studied. Using 20 wt.% Na_2CO_3 doping, the vitrification temperature can be reduced to 1200°C. Under this condition, amorphous glass phases were homogeneously distributed in the sintered samples. As the Na_2CO_3 content increased, the density of the sample sintered at 1200°C increased from 1.39 g/cm^3 to 2.24 g/cm^3 initially and then increased to 2.40 g/cm^3 with elevated Na_2CO_3 content. The density increase tendency gradually became slow from 1200°C to 1300°C. The Vickers hardness exhibited a similar tendency with the density. The hardness reached a relatively high value of 781 HV and 823 HV for the samples with the addition of 20 wt.% Na_2CO_3 sintered at 1200°C and 1300°C, respectively. The uranium tailings mixture doped 20 wt.% Na_2CO_3 sintered at 1200°C showed excellent performance, regardless of the density or Vickers hardness. It can be concluded that the introduction of Na_2CO_3 was verified to be instrumental to reduce the sintering temperature and enhance the densification of the vitrified forms. It indicated that the combination of microwave sintering with the appropriate addition of Na_2CO_3 would provide an efficient method for the immobilization of radionuclides in uranium tailings.

Data Availability

The data used to support the findings of this study are included within the supplementary information file.

Additional Points

This paper is an experimental study on glass solidified uranium tailings based on microwave sintering. Uranium tailings, surface cladding, Na_2CO_3, and alcohol were mixed and stirred well in an agate mortar. The glass matrix with a smooth surface and good mechanical properties was prepared by a microwave muffle furnace.

Conflicts of Interest

The authors declare that they have no known competing financial interests or personal relationships that could have appeared to influence the work reported in this paper.

Authors' Contributions

First author Wei Wei and second author Keyou Shi contribute equally to the article.

Acknowledgments

The authors appreciate the financial supports from the Research and Development Program in Key Areas of Hunan Province (no. 2019SK2011), Hunan Provincial Innovation Foundation For Postgraduate (no. CX20190711), the National Natural Science Foundation of China (no. 11875164), the Decommissioning of Nuclear Facilities and Radioactive Waste Treatment Project of National Defense Science and Industry Administration (no. JSZL2019403C001), "Thirteenth Five-Year Plan" Technology Basic Research Project of National Defense Science and Industry (nos. JSZL2017403B008 and JSZL2018403B001), Equipment Pre-Research Project of the Equipment Development Department of the Central Military Commission (no. 32104060202), and Military and Civil Integration Project in Hunan Province (no. 200GJM001).

Supplementary Materials

The document "graphical abstract.doc" is a graphical abstract of the manuscript. "XRF.txt" is the original data file of Table 1. "Power and Temperature.txt" is the raw data file of Figure 1. "XRD.txt" is the raw data file of Figure 3. "FTIR.txt" is the raw data file of Figure 4. "SEM and EDS.doc" is the raw data file of Figure 5. "Density and porosity.txt" is the raw data file of Figure 6. "Vickers hardnessd.txt" is the raw data file of Figure 7. (*Supplementary Materials*)

References

[1] F. Luo, H. Tang, X. Shu et al., "Immobilization of uranium-contaminated soil into glass waste by microwave sintering: experimental and theoretical study," *Journal of Non-crystalline Solids*, vol. 556, Article ID 120551, 2020.

[2] S. Chen, X. Shu, H. Tang, X. Mao, C. Xu, and X. Lu, "Microwave vitrification of uranium-contaminated soil for nuclear test site and chemical stability," *Ceramics International*, vol. 45, no. 10, pp. 13334–13339, 2019.

[3] A. O. Aidarkhanov, S. N. Lukashenko, O. N. Lyakhova et al., "Mechanisms for surface contamination of soils and bottom sediments in the Shagan River zone within former Semipalatinsk Nuclear Test Site," *Journal of Environmental Radioactivity*, vol. 124, pp. 163–170, 2013.

[4] Y. Liu, W. Zhou, H. Liu, Q. Wei, B. Gao, and G. Chen, "Spatial variability and radiation assessment of the radionuclides in soils and sediments around a uranium tailings reservoir, south of China," *Journal of Radioanalytical and Nuclear Chemistry*, vol. 324, no. 1, pp. 33–42, 2020.

[5] H. Tuovinen, E. Pohjolainen, D. Vesterbacka et al., "Release of radionuclides from waste rock and tailings at a former pilot uranium mine in eastern Finland," *Boreal Environment Research*, vol. 21, no. 5-6, pp. 471–480, 2016.

[6] J. Wang, J. Liu, H. Li et al., "Surface water contamination by uranium mining/milling activities in Northern Guangdong province, China," *CLEAN-Soil, Air, Water*, vol. 40, no. 12, pp. 1357–1363, 2012.

[7] M. Al-Zoughool and D. Krewski, "Health effects of radon: a review of the literature," *International Journal of Radiation Biology*, vol. 85, no. 1, pp. 57–69, 2009.

[8] X. Nie, D. Ding, and G. Li, "Soil radionuclide contamination and radionuclide accumulation characteristics of competitive

plants in a uranium tailings repository in South China," *Environmental Research*, vol. 23, pp. 719–725, 2010.

[9] X. Mao, R. Jiang, W. Xiao, and J. Yu, "Use of surfactants for the remediation of contaminated soils: a review," *Journal of Hazardous Materials*, vol. 285, pp. 419–435, 2015.

[10] M. Gavrilescu, L. V. Pavel, and I. Cretescu, "Characterization and remediation of soils contaminated with uranium," *Journal of Hazardous Materials*, vol. 163, no. 2-3, pp. 475–510, 2008.

[11] G.-N. Kim, I. Kim, S.-S. Kim et al., "Removal of uranium from contaminated soil using indoor electrokinetic decontamination," *Journal of Radioanalytical and Nuclear Chemistry: An International Journal Dealing with All Aspects and Applications of Nuclear Chemistry*, vol. 309, no. 3, 2016.

[12] X. Li, J. Wu, J. Liao et al., "Adsorption and desorption of uranium (VI) in aerated zone soil," *Journal of Environmental Radioactivity*, vol. 115, pp. 143–150, 2013.

[13] S. Landsberger, D. Tamalis, T. Meadows, and B. Clanton, "Leaching dynamics of uranium in a contaminated soil site," *Journal of Radioanalytical and Nuclear Chemistry*, vol. 296, no. 1, pp. 319–322, 2013.

[14] S. S. Kim, G. S. Han, G. N. Kim, D. S. Koo, I. G. Kim, and J. W. Choi, "Advanced remediation of uranium-contaminated soil," *Journal of Environmental Radioactivity*, vol. 164, pp. 239–244, 2016.

[15] I. Sánchez-Castro, A. Amador-García, C. Moreno-Romero et al., "Screening of bacterial strains isolated from uranium mill tailings porewaters for bioremediation purposes," *Journal of Environmental Radioactivity*, vol. 166, pp. 130–141, 2016.

[16] G.-N. Kim, S.-S. Kim, H.-M. Park, W.-S. Kim, U.-R. Park, and J.-K. Moon, "Remediation of soil/concrete contaminated with uranium and radium by biological method," *Journal of Radioanalytical and Nuclear Chemistry*, vol. 297, no. 1, pp. 71–78, 2013.

[17] V. N. Jha, R. M. Tripathi, N. K. Sethy, and S. K. Sahoo, "Uptake of uranium by aquatic plants growing in fresh water ecosystem around uranium mill tailings pond at Jaduguda, India," *Science of the Total Environment*, vol. 539, pp. 175–184, 2016.

[18] E. Coelho, T. A Reis, M. Cotrim, M. Rizzutto, and B. Corrêa, "Bioremediation of water contaminated with uranium using Penicillium piscarium," *Biotechnology Progress*, vol. 36, no. 5, p. e30322, 2020.

[19] W. Zhang and J. Wang, "Leaching performance of uranium from the cement solidified matrices containing spent radioactive organic solvent," *Annals of Nuclear Energy*, vol. 101, pp. 31–35, 2017.

[20] J. Dragun, "Geochemistry and soil chemistry reactions occurring during in situ vitrification," *Journal of Hazardous Materials*, vol. 26, no. 3, pp. 343–364, 1991.

[21] G. Guo, Q. Zhou, and L. Q. Ma, "Availability and assessment of fixing additives for the in situ remediation of heavy metal contaminated soils: a review," *Environmental Monitoring and Assessment*, vol. 116, no. 1-3, pp. 513–528, 2006.

[22] F. W. Münscher, "Radionuclides containment in nuclear glasses: an overview," *Radiochimica Acta*, vol. 105, no. 11, pp. 927–959, 2017.

[23] H. Tang, Y. Li, W. Huang et al., "Chemical behavior of uranium contaminated soil solidified by microwave sintering," *Journal of Radioanalytical and Nuclear Chemistry*, vol. 322, no. 3, pp. 2109–2117, 2019.

[24] C. P. Kaushik, R. K. Mishra, P. Sengupta et al., "Barium borosilicate glass–a potential matrix for immobilization of sulfate bearing high-level radioactive liquid waste," *Journal of Nuclear Materials*, vol. 358, no. 2-3, pp. 129–138, 2006.

[25] D. R. Dixon, M. J. Schweiger, B. J. Riley, R. Pokorny, and P. Hrma, "Temperature distribution within a cold cap during nuclear waste vitrification," *Environmental Science & Technology*, vol. 49, no. 14, pp. 8856–8863, 2015.

[26] J. S. Mccloy, B. J. Riley, A. Goel et al., "Rhenium solubility in borosilicate nuclear waste glass: implications for the processing and immobilization of technetium-99," *Environmental Science & Technology*, vol. 46, no. 22, pp. 12616–12622, 2012.

[27] Y. Orooji, M. R. Derakhshandeh, E. Ghasali, M. Alizadeh, M. Shahedi Asl, and T. Ebadzadeh, "Effects of ZrB2 reinforcement on microstructure and mechanical properties of a spark plasma sintered mullite-CNT composite," *Ceramics International*, vol. 45, no. 13, pp. 16015–16021, 2019.

[28] Y. Orooji, A. a. Alizadeh, E. Ghasali et al., "Co-reinforcing of mullite-TiN-CNT composites with ZrB2 and TiB2 compounds," *Ceramics International*, vol. 45, no. 16, pp. 20844–20854, 2019.

[29] J. P. Robinson, S. W. Kingman, C. E. Snape, H. Shang, R. Barranco, and A. Saeid, "Separation of polyaromatic hydrocarbons from contaminated soils using microwave heating," *Separation and Purification Technology*, vol. 69, no. 3, pp. 249–254, 2009.

[30] S. Mengyong, L. Qinggang, H. Shifeng, and C. Xin, "The densification of Si3N4 ceramics using different additives via microwave sintering," *Journal of the Ceramic Society of Japan*, vol. 122, no. 1430, pp. 914–916, 2014.

[31] P. M. Souto, R. R. Menezes, and R. H. G. A. Kiminami, "Effect of Y2O3 additive on conventional and microwave sintering of mullite," *Ceramics International*, vol. 37, no. 1, pp. 241–248, 2011.

[32] J. Duan, Z. Huang, C. Shi et al., "Effect of MgO doping on densification and grain growth behavior of Gd2Zr2O7 ceramics by microwave sintering process," *Applied Physics A*, vol. 125, no. 8, pp. 556.1–556.7, 2019.

[33] S. Zhang, X. Shu, S. Chen et al., "Rapid immobilization of simulated radioactive soil waste by microwave sintering," *Journal of Hazardous Materials*, vol. 337, pp. 20–26, 2017.

[34] T. Petit and L. Puskar, "FTIR spectroscopy of nanodiamonds: methods and interpretation," *Diamond and Related Materials*, vol. 89, pp. 52–66, 2018.

[35] M. A. Vicente-Rodríguez, M. Suarez, M. A. Bañares-Muñoz, and J. de Dios Lopez-Gonzalez, "Comparative FT-IR study of the removal of octahedral cations and structural modifications during acid treatment of several silicates," *Spectrochimica Acta Part A: Molecular and Biomolecular Spectroscopy*, vol. 52, no. 13, pp. 1685–1694, 1996.

[36] Z. Huang, Z. Cao, K. Shi et al., "Synthesis and densification of Gd 2 Zr 2 O 7 nanograin ceramics prepared by field assisted sintering technique," *Journal of Nuclear Materials*, vol. 495, pp. 164–171, 2017.

[37] D. Ma, Z. Kou, Y. Liu et al., "Sub-micron binderless tungsten carbide sintering behavior under high pressure and high temperature," *International Journal of Refractory Metals & Hard Materials*, vol. 54, 2016.